Vibrational circular dichroism of a 2,5-diketopiperazine (DKP) peptide: Evidence for dimer formation in cyclo LL or LD diphenylalanine in the solid state

Ariel Pérez-Mellor, Anne Zehnacker

Vibrational Circular Dichroism of a 2,5-Diketopiperazine (DKP) Peptide: Evidence for Dimer Formation in cyclo LL or LD diphenylalanine in the solid state

Ariel F. Pérez -Mellor,[a] Anne Zehnacker*[a]

Keywords: FTIR spectroscopy - Vibrational Circular Dichroism -VCD - peptide - Diketopiperazine - DKP - hydrogen bond

Abstract: The diastereomer diketopyperazine (DKP) peptides built on phenylalanine, namely, cyclo diphenylalanine LPhe-LPhe and LPhe-DPhe, have been studied in the solid phase by Vibrational Circular Dichroism (VCD) coupled to quantum chemical calculations. The unit structure of cyclo LPhe-LPhe in KBr pellets is a dimer bridged by two strong NH…O hydrogen bonds. The intense bisignate signature in the CO stretch region is interpreted in terms of two contributions arising from the free COs of the dimer and the antisymmetrical combination of the bound COs. In contrast, cyclo LPhe-DPhe shows no VCD signal in relation with its symmetric nature.

Introduction

Homochirality is pervasive in life chemistry. It plays a major role in the structure of biomolecules, which are, for most of them, composed of elementary blocks of the same handedness. Cornerstone examples are peptides and proteins, which are built from naturally-occurring L amino-acids. Exceptions to homochirality, resulting for example from post translational modifications,[1,2] have important consequences in the function of biomolecules, due to a change in both intra and intermolecular interactions, for example in protein folding[3] or activity.[4] These changes are often related to a change in the biopolymer structure, as observed in the Trp-cage mini-protein, the structure of which is strongly modified by the change of chirality of a single amino-acid.[5]

The effects of modifying the handedness of one monomer in a biopolymer have been studied at the molecular level in model systems, both neutral molecules as well as protonated or sodiated species.[6-10] Although often weak in short neutral or protonated peptides, the effects are more pronounced in long protonated poly-alanine strands whose helical shape is disrupted when reverting the chirality of one residue,[11] in sodiated peptides,[10,12,13] or in cyclically constrained β-peptides with chirality-dependent intramolecular hydrogen bonding pattern.[9] Solution-phase studies of the way diastereomerism impinges the structure of peptides rely on various structure-sensitive techniques such as NMR,[14] and vibrational spectroscopy.[15,16] Of special interest are the chiroptical methods like Vibrational Circular Dichroism (VCD)[17-22] or Raman Optical Activity (ROA).[23-25] VCD is indeed very sensitive to minute conformational changes,[26,27] hence a very good probe of molecular conformation.[28,29] It has been widely applied to peptides, as a powerful tool for determining their secondary structure, in particular in the Amide I (C=O stretch) region.[30-36] [37-39] β-sheets and coils have for example different amide I spectra from that of the α-helix.[40] VCD is also very sensitive to the aggregation state and allows the characterisation of various size entities ranging from dimers [41] to β-sheets or fibrils formation,[42] as well as self-assemblies in solution or in the solid state.[43]

Diketopyperazine (DKP) peptides are an important class of dipeptides with applications in pharmacology as HIV antiviral drugs, or anticancer therapy.[44-47] The DKP ring also is a decomposition product of the well-known sweetener aspartame or dipeptide drugs.[48-50] These cyclic dipeptides result from the intramolecular peptide coupling of a linear α dipeptide, with concomitant dehydration.[51-53] They have been the subject of many conformational studies, since the first elucidation of their crystal structure.[54] The DKP ring may indeed adopt several conformations depending on the nature of the residues, with either planar, boat, or chair conformation of the ring. While it remains planar for very small residues like glycine, it undergoes an out of plane distortion for those that are bulkier, with pseudo axial or pseudo equatorial position of the substituents.[55] Bulky residues like phenylalanine or tyrosine often adopt a so-called flagpole position,[56,57] unless steric hindrance decides otherwise. Indeed, when the DKP peptide contains two bulky substituents, it also appears that one of them is folded over the ring while the second one is extended.[58] DKP dipeptides have restricted conformational freedom, a fact that provides useful model systems for the study of electronic or vibrational coupling between the two residues. Indeed, the question has been raised as to whether the electronic transitions located on the two residues are coupled, if this coupling depends on the ring geometry, and if it can be evidenced in electronic circular dichroism using the so-called exciton coupling model.[59] [60,61] From a vibrational point of view as well, DKP dipeptides allow probing the coupling between the Amide I and II modes in a system of well-defined geometries. This will allow shedding light on the factors that defines the band shapes in IR absorption and VCD in systems that show several amide modes potentially coupled.[38] [62-65] Like in electronic circular dichroism,

[a] *Mr A.F. Pérez-Mellor, Dr. A. Zehnacker Author(s)*
Institut des Sciences Moléculaires d'Orsay (ISMO), CNRS and Univ Paris-Sud, Orsay, F-91405, France.
Fax: (+) 33 1 69 15 67 77
E-mail: anne.zehnacker-rentien@u-psud.fr

Received: ((will be filled in by the editorial staff))
Revised: ((will be filled in by the editorial staff))
Published online: ((will be filled in by the editorial staff))

coupling between two vibration modes has been proposed to interpret the bisignate signature observed, which consists of two bands of opposite sign.[62] However, bisignate band shapes can also be accounted for by the presence of several conformers, with close-lying absorption bands with opposite VCD.[64] A generalised coupled oscillator (GCO) model has been recently proposed to interpret the shape of VCD spectra in both symmetrical and asymmetric molecules.[66]

We have undertaken the study of dipeptides with identical or opposite chirality, both in the gas phase and in the condensed phase, with the aim of understanding how homo or heterochirality of the residues impinges their structure and can be identified by its spectroscopic signature.[10,67] We shall focus here on cyclo diphenylalanine, denoted cyclo Phe-Phe hereafter, which has attracted special attention due to its spontaneous formation by heating the parent Phe-Phe linear dipeptide.[68,69] Both cyclo LPhe-LPhe and cyclo LPhe-DPhe will be studied in the solid phase. The presence of bulky aromatic rings is expected to introduce steric constraints and to increase stabilizing dispersive interactions within the peptide.[70,71] Last, the Phe aromatic rings can act as weak hydrogen bond acceptors. The molecules under study are shown in Figure 1.

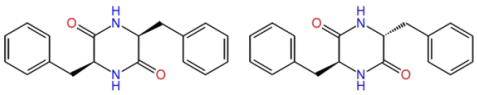

FIGURE 1 Molecules under study. Left: cyclo LPhe-LPhe. Right: cyclo LPhe-DPhe.

Materials and Methods

EXPERIMENTAL SET-UP

The vibrational IR absorption and VCD spectra were measured using a FTIR spectrometer (Vertex 70 Bruker) equipped with a VCD module (PMA 50 Bruker). The signal was measured by a MCT IR detector with a BaF_2 window, cooled with liquid nitrogen. A spectral resolution of 4 cm^{-1} was used for both absorption and VCD spectra in the fingerprint region. The absorption spectra were repeated over the whole 800–3700 cm^{-1} range at a 1 cm^{-1} resolution. The IR radiation was first polarized with a linear polarizer then modulated by a 50 kHz ZnSe photoelastic modulator (Hinds). A low-pass filter cutting at 2000 cm^{-1} was added before the linear polarizer to increase the dynamical response of the detector when measuring the fingerprint region. The signal of the MCT detector was demodulated using a lock-in amplifier (Stanford Research Systems SR 830). The alignment of the spectrometer was carefully checked by checking the mirror-image relation between the VCD spectra of the two enantiomers of camphor (0.3M in CCl_4). The samples were prepared by grinding 10mg of molecule and 3.5g of KBr in a mixer mill (MM 400 Retsch) at 20Hz during 1hr. The samples were then gently heated at 80°C to eliminate most of the water. The artefacts due to the birefringence of the KBr pellets were eliminated by following the procedure proposed by Merten,[72] derived from that introduced by Buffeteau.[73] It consists in rotating the sample in the plane perpendicular to the light propagation axis for each side (front F or back B) of the pellet and averaging the spectra obtained for each position of the pellet at 0° and 90°. For the sake of better averaging and artefact control, the procedure has been extended to 180° and 270°. The measure was obtained by adding 4200 scans for each sample position.

$$\mathrm{I}^{\mathrm{VCD}}(\tilde{\nu}) = \frac{1}{8}\sum_{n=0}^{3} \mathrm{I}^{\mathrm{VCD}}(\tilde{\nu}; n \cdot 90°; \mathrm{F}) + \mathrm{I}^{\mathrm{VCD}}(\tilde{\nu}; n \cdot 90°; \mathrm{B})$$

The dipeptides were purchased from GeneCust-Luxembourg (98% purity) and used without further purification.

THEORETICAL METHODS

A first exploration of the potential energy surface was performed for both diastereomers using the Macromodel program included in the Maestro suite.[74] The conformational mobility is limited by the cyclic nature of the system, and only ~10 different monomers were calculated with energy within 21kJ/mol with the OPLS_2005 force field used. They were further optimized at the B3LYP/6-311++g(d,p) level of theory, including the D3 empirical dispersion factor, using Gaussian 09.[75,76] The vibrational IR absorption and circular dichroism spectra were simulated by calculating the harmonic frequencies at the same level of theory and convoluting the scaled frequencies by a Lorentzian line shape of 8 cm^{-1} FWMH, chosen to reproduce the experimental bandwidth. The calculated frequencies were scaled by 0.952. This scaling factor gives indeed a good agreement between the experimental and calculated amide stretch A of cyclo Phe-Phe in the gas phase.[67] The stability of the monomer is given in terms of Gibbs energy ΔG at 298.15 K (in kcal/mol) relative to the most stable conformation.

No significant change was observed in the relative stability nor in the calculated IR and VCD spectra of the monomers when using the smaller basis set 6-31g(d,p), as shown in Table S1 and Figure S1 of the supporting information. The 6-31g(d,p) basis set was therefore used for the dimers; the same procedure was followed, using the same scaling factor as for the monomers.

Results and Discussion

EXPERIMENTAL RESULTS

The IR absorption spectra of the two diastereomers are shown in Figure 2. They display a similar pattern in the Amide I and II region, with an intense feature centred around 1670 cm^{-1}, readily assignable to the C=O stretch. This feature is composed of a doublet in cyclo LPhe-LPhe at 1663-1677 cm^{-1} while it is a single band located at 1677 cm^{-1} in cyclo LPhe-DPhe, with however a shoulder in the low-energy side that shows that it corresponds to the superposition of two bands. The Amide II (β(NH) bend) region of cyclo LPhe-LPhe displays a broad feature with two maxima at 1462 cm^{-1} and 1454 cm^{-1}, and a side band at 1498 cm^{-1}. In cyclo LPhe-DPhe, similar features are observed. However, the cyclo LPhe-DPhe spectrum extends slightly more, with additional side bands at 1440 and 1486 cm^{-1}. The hydride stretch region shows a complicated pattern resulting from the superposition of the 14 ν(CH) stretches, and two bands assigned to the ν(NH) stretches at 3205 / 3316 cm^{-1} and 3189 /3326 cm^{-1} for cyclo LPhe-LPhe and cyclo LPhe-DPhe, respectively. One can deduce from the similitude between the absorption spectra that similar structures exist for cyclo LPhe-LPhe and cyclo LPhe-DPhe. Their shape, in particular the presence of two ν(NH) bands with different frequencies, indicates that the sample contains NH groups in two sorts of local environment. Similarly, the doublet observed in the ν(CO) stretch region of cyclo LPhe-LPhe indicates that the cyclo LPhe-LPhe sample contains CO groups in at least two distinct local environments.

The experimental VCD spectra recorded in the fingerprint region are shown in Figure 3. They totally differ from each other. While cyclo LPhe-LPhe shows intense VCD signal in the ν(CO) stretch region, of the order of $3.5 \cdot 10^{-4}$, and weaker bands in the β(NH) bend region, no signal is detected for cyclo LPhe-DPhe in the same experimental conditions, which easily allow detecting signals down to 10^{-5}. The absence of signal for cyclo LPhe-DPhe might arise from different possibilities, including centrosymmetric structures, which will be discussed later.

The cyclo LPhe-LPhe spectrum is characterised by a bisignate signature in the ν(CO) region, with an intense positive peak at low energy followed by a negative peak of similar intensity, a point to which we shall return in the discussion. The broad β(NH) band at 1454/1462 cm^{-1} also shows a bisignate signature, although of opposite sign and much weaker intensity than that due to the ν(CO) stretches.

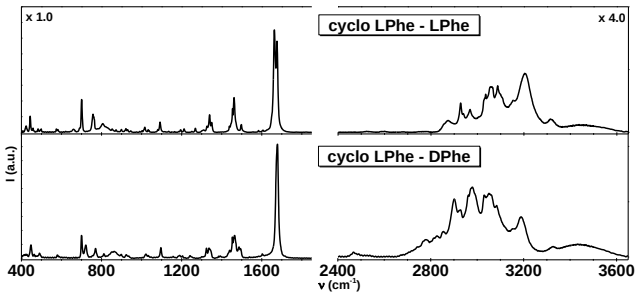

FIGURE 2 Experimental infrared absorption spectra, recorded at a resolution of 1 cm^{-1}. Top: cyclo LPhe-LPhe. Bottom: cyclo LPhe-DPhe. The intensity in the region of the hydride stretch has been multiplied by 4.

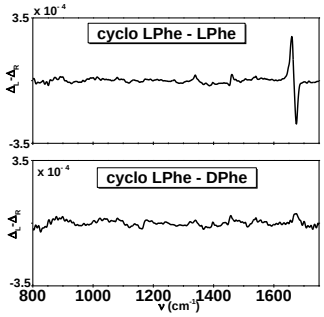

FIGURE 3 Experimental VCD spectra in the fingerprint region, recorded at a resolution of 4 cm^{-1}. Top: cyclo LPhe-LPhe. Bottom: cyclo Lphe-DPhe.

THEORETICAL RESULTS

Calculated structures and assignment for cyclo LPhe-LPhe

The experimental IR spectrum of cyclo LPhe-LPhe has been compared first to that simulated for the most stable calculated structure cLL-A, which is the conformer observed in the gas phase in jet-cooled conditions.[67] This structure is very close to that observed in the cyclo LPhe-LPhe crystal, with one Phe folded over the DKP ring and the other one extended.[77] Only a mild agreement is obtained for the IR spectrum, as shown in Figure 4. In particular, the energy gap between the amide I and II bands is by far too large in the calculated spectrum; this is the case for all the calculated monomers. Moreover, the calculated VCD spectrum of the most stable structure fails to reproduce the bisignate signature. A bisignate signature is only obtained in symmetrical structures such as cLL-D and cLL-E, shown in Figure 4, with however the wrong sign.

The existence of dimers could explain the observation of two different ν(CO) and two different ν(NH) bands. The most stable calculated $(cLL)_2$-I dimer satisfactorily reproduces the experimental spectroscopic results (see Figure 5). The most stable $(cLL)_2$-I dimer displays two strong hydrogen bonds bridging the CO and NH groups of the two subunits, with CO···HN distances as short as 1.81 Å. Due to the steric hindrance induced by the aromatic rings, the double hydrogen bridge shows a small deviation from planarity (ONON dihedral of 8°). The DKP geometry in both monomers consists in a flattened boat with the C_β atoms in pseudoaxial positions. The deviation from planarity of the DKP ring is weak. The calculated CCNC dihedral amounts indeed to -14° in the dimer *vs*. -12° in the gas phase monomer. This value is very close to that measured in the crystal (-11°).[67,77] The small difference between the monomer and the dimer is not significant and might result from differences in the methods used. Interestingly, the two subunits are not totally identical to each other, which results to a slightly asymmetric hydrogen bond bridge with one hydrogen bond farther to linearity (165°) than the other (175°). One of the two moieties is similar to that observed in the gas phase and in the crystal, with one aromatic ring bent over the DKP ring in a "flag pole" position while the other one is in an extended position.[77] This structure corresponds to NCCC dihedral angles of -58° for the extended Phe and 65° for the folded one. The second subunit is much more symmetrical with Phe substituents located on the same side of the DKP ring, as often observed when the two residues interact with each other.[78] The corresponding dihedral angles are 73° and 59°, respectively. Such a structure allows Phe-Phe stacking interaction to take place, similar to what is observed in cyclo LArg-LTrp.[30] This contrasts with what is observed in the neat crystal, in which all the monomers have an identical structure.[77] It should be noted that attempts at reproducing the VCD spectrum with a symmetrical structure identical to the crystal sub-unit and optimised in the gas phase failed, as shown in Figure S2 of the supporting information.

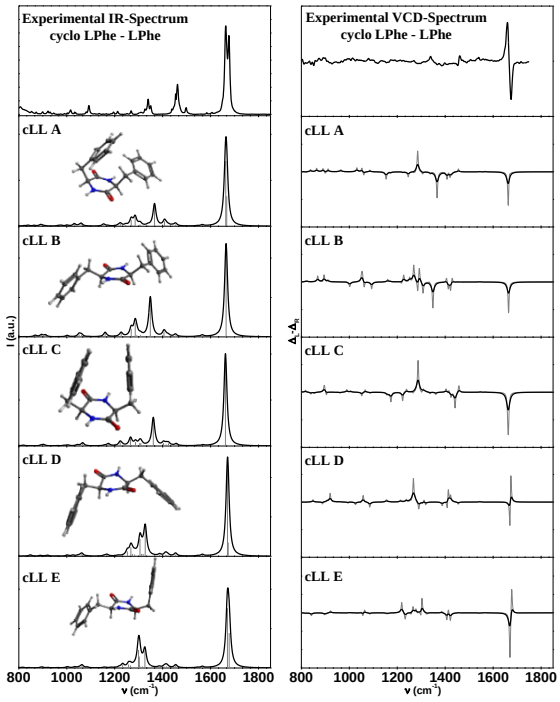

FIGURE 4 Comparison between experimental and simulated IR and VCD spectra in the fingerprint region for the most stable monomers of cyclo LPhe-LPhe at the DFT-D3/B3LYP/6-311++G(d,p) level of theory. The simulated spectra were obtained by convoluting the harmonic frequencies by a Lorentzian shape with a FWHM=8 cm^{-1}.

As both free and bound ν(CO) and ν(NH) stretching modes appear in the experimental spectrum, its interpretation in terms of trimers, tetramers, or larger oligomers of cyclo LPhe-LPhe cannot be ruled out. Information can be gained however from the comparison between the relative intensity of the doublet experimentally observed in the ν(CO) stretch region and the shape of the spectrum calculated for clusters of different sizes. For the sake of computational efficiency, we have optimised the structures of monomers, dimers, trimers and tetramers of the model system (LL) cyclo Ala-Ala, at the B3LYP/6-31g(d,p) level of theory. The simulated spectra, displayed in Figure S3 of the supporting information, show that the calculated intensity ratio between the high-energy and low-energy components of the doublet decreases when the cluster size increases. This ratio reflects indeed the ratio between free (high energy band) and bound (low energy band) CO groups, which scale like (*n*-1), *n* being the number of units in the oligomer. The best agreement with the experiment is clearly obtained with the dimer structure, which shows similar intensities for the two components of the doublet as experimentally observed. This observation allows ruling out the existence of a long oligomeric chain of cyclo LPhe-LPhe.

FIGURE 5 Comparison between experimental and simulated IR

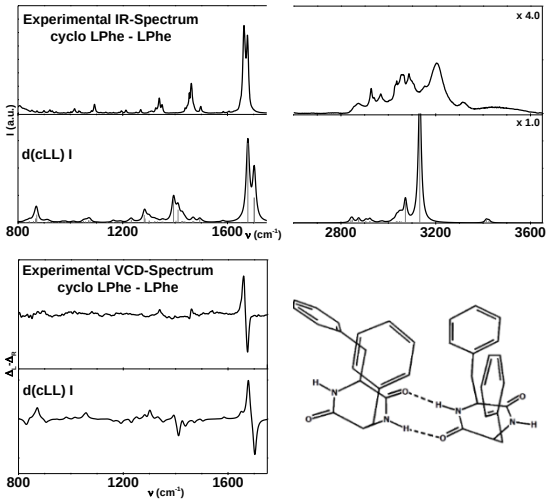

spectra of the most stable dimer $c(LL)_2$-I of cyclo LPhe-LPhe. Bottom: Comparison between experimental and simulated VCD spectra of $c(LL)_2$-I. Most stable calculated structure $c(LL)_2$-I. The simulated spectra were obtained by convoluting the harmonic frequencies by a Lorentzian line shape with a 8 cm^{-1} FWHM.

Frequency analysis for the cyclo LPhe-LPhe dimer

The main observed vibrational bands are collected in Table 1, together with the calculated frequencies, IR absorption intensities, oscillator strengths, and proposed assignment. In the calculated $(cLL)_2$-I dimer, the free ν(NH) stretches are not coupled to each other, nor are the free ν(CO) stretches, which appear as the high-energy component of the doublet experimentally observed at 1662-1678 cm^{-1}. The two free ν(CO)s have a negative VCD signal that both contribute to the observed negative component of the bisignate doublet. The bound CO stretches are strongly coupled together, which results in a strongly allowed asymmetric combination and an almost completely forbidden, symmetric, one. The allowed ν(CO) has a strong positive VCD signal while that of the forbidden ν(CO) is zero. The bisignate signature observed in the ν(CO) region is therefore not due to exciton coupling but to superimposed contributions of different ν(CO)s. Like the bound ν(CO) stretches, the bound β(NH) bends are strongly coupled to each other. They appear however weakly in the spectrum due to limited oscillator strength. In contrast to the free stretches, the free β(NH) bends are strongly coupled to each other and to the β(CH) or $β(CH_2)$ bends. They appear as a bisignate doublet in the VCD spectrum at 1452 and 1462 cm^{-1}. In conclusion, the two bisignate doublets which appear in the VCD spectrum of cyclo LPhe-LPhe have completely different origins: while the weak-intensity bisignate signature around 1450 cm^{-1} is due to exciton coupling, the strong one around 1670 cm^{-1} is due to ν(CO)s in different environments, which show contributions of opposite sign.

TABLE 1 Frequencies assignment for cyclo LPhe-LPhe. (*) The theoretical frequencies are not scaled. The position of experimental frequencies was determined using the second derivative criterion.

Calculated structures and assignment for cyclo LPhe-DPhe

The case of cyclo LPhe-DPhe is more delicate to interpret as no VCD signal is observed. The presence of a single feature in the ν(CO) stretch region might suggest the presence of monomers. However, the calculated monomer structures do not reproduce the experimental IR spectrum, in particular in the region of the ν(NH) stretch, where both free and bound NH appear. Moreover, all of them display non zero VCD spectrum (see Figure S4 of the supporting information). We therefore calculated the cyclo LPhe-DPhe dimers, as we did for cyclo LPhe-LPhe. There are two possibilities for obtaining a system with no optical activity. The first one is the co-existence of two enantiomers with opposite VCD spectra that cancel out, a point to which we shall return later.

The second possibility is the formation of a centrosymmetric dimer, for example the calculated $(cLD)_2$-sym dimer shown in Figure 6a). It displays the same double hydrogen bridge pattern as the cyclo LPhe-LPhe dimer. However, the stereochemistry of cyclo LPhe-DPhe allows for the formation of a centrosymmetric dimer with no optical activity. This is an example of what is called "la coupe du roi", a non-chiral system built from two chiral moieties of opposite chirality,[79] a phenomenon also observed in a jet-cooled isolated dimer.[80]

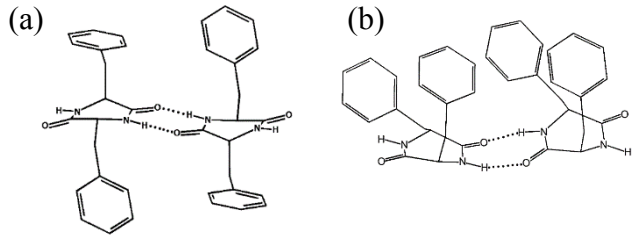

FIGURE 6 a) Centrosymmetric structure $c(LD)_2$-sym of the cyclo LPhe-DPhe dimer. b) Most stable structure $c(LD)_2$-I of the cyclo LPhe-DPhe dimer.

This centrosymmetric dimer is however not the most stable one; its relative energy amounts to 1.77 kcal/mol relative to the most stable form. The most stable dimers obtained after the exploration and optimization steps belong to the C_1 symmetry point group, due to the position of the Phenylalanine residues. As seen for the most stable of them ($(cLD)_2$-I shown in Figure 6b), a weak CH-π interaction takes place between the $C_\alpha H$ of one of the residues and the benzene ring of the other, which breaks the symmetry of the system. As cyclo LPhe-DPhe contains identical Phe residues, which differ by nothing but their chirality, it is not possible to distinguish which of LPhe or DPhe aromatic ring acts as a hydrogen bond acceptor and which is "free". For this reason two transient enantiomers are expected for cyclo LPhe-DPhe, namely cyclo LPhe(donor)-DPhe(acceptor) and cyclo DPhe(donor)-LPhe(acceptor). They show equal populations hence contributions to the IR absorption spectrum, shown in Figure S5, and opposite contributions to the VCD spectrum. Switching from one of the transient enantiomers to the other corresponds to a switch between "free" and "H-bonded" aromatic rings. The enantiomers can formally be seen as cyclo LPhe(donor)-DPhe(acceptor) and cyclo DPhe(donor)-LPhe(acceptor), but the asymmetric carbons themselves of course do not change chirality. What physically happens is that LPhe(donor) changes to LPhe(acceptor). This process does not involve cleavage and formation of chemical bonds but inversion of the DKP ring and rotation of the phenethyl substituents. A possible reaction path has been calculated between the two transient enantiomers of the lower-energy cyclo LPhe-DPhe monomer and is shown in Figure S6. The calculated transition state is centrosymmetric and corresponds to a barrier of 2.1 kcal/mol only. Although these calculations are carried out in the gas phase, we expect that interconversion between the two transient enantiomers also happens during the sample preparation.

On the basis of the experimental finding, it is not possible to decide between the two possibilities, either centrosymmetric dimer, or two transient enantiomers. We tend to favour the second one because the calculated structure is lower in energy in the gas phase. However, the energy ordering could be modified in the condensed phase.

Conclusion

The two diastereomers of cyclo diphenylalanine has been studied in the solid state, in order to shed light on its aggregation state when embedded in KBr pellets. To this end, samples of finely grinded cyclo LPhe-LPhe and cyclo LPhe-DPhe in KBr have been studied by IRTF as well as VCD spectroscopy, combined with quantum chemical calculations. For simple

aromatic molecules like 1H-indazoles, it has been proposed that calculations resting on a description of the system in terms of a small cluster that reflects the elementary cell give satisfactory agreement with the experimental VCD spectrum, for both band position and sign.[43] In the cyclo LPhe-LPhe studied here however, the sample does not exist in the form it possesses in crystals, namely, infinite chains involving molecular units bridged by two NH…O hydrogen bonds. Here, the unit cell is the dimer, as can be deduced from the observation of both bound and free ν(CO) and ν(NH) stretches. The DKP geometry in both monomers consists in a flattened boat with the C_β atoms in pseudoaxial positions, with a deviation from planarity of the DKP ring of the same order as in the gas phase or the crystal.[67,77] The two moieties of the dimer are not equivalent in terms of phenyl ring arrangement, which contrasts to the neat solid. Such a dissymmetry has been observed already for supramolecular structures in solution; for example the tetramer of a chiral dicarboxylic acid is composed of three identical monomers plus one.[81] This structure accounts well for the bisignate signatures observed in the ν(CO) and β(NH) regions of the VCD spectrum. The higher-energy positive component of the intense doublet observed in the ν(CO) region has been assigned to the superimposed contribution of the two free ν(CO) stretches while the lower-energy negative component has been assigned to the antisymmetric combination of the bound ν(CO) stretches. In contrast, the two components of the much weaker bisignate signature observed in the β(NH) range are due to the symmetric and asymmetric combinations of the bound β(NH) bends, respectively. Dimers of rigid DKP peptides provide therefore interesting systems for studying the effects of mode coupling due to transition dipole coupling (TDC) as well as through-bond effects, including hydrogen bonds. Other DKP dipeptides are currently under study both in the gas and in the solid phases.

Acknowledgements

We acknowledge the use of the computing facility cluster GMPCS of the LUMAT federation (FR LUMAT 2764).

Supporting information

Additional supporting information may be found in the online version of this article at the publisher's website.

REFERENCES AND NOTES

1. Buczek O, Yoshikami D, Bulaj G, Jimenez EC, Olivera BM. Post-translational amino acid isomerization - A functionally important D-amino acid in an excitatory peptide. *Journal of Biological Chemistry* **2005**;280(6):4247-4253.
2. Cotter PD, O'Connor PM, Draper LA, Lawton EM, Deegan LH, Hill C, Ross RP. Posttranslational conversion of L-serines to D-alanines is vital for optimal production and activity of the lantibiotic lacticin 3147. *Proceedings of the National Academy of Sciences of the United States of America* **2005**;102(51):18584-18589.
3. Kwiecinska JI, Cieplak M. Chirality and protein folding. *Journal of Physics-Condensed Matter* **2005**;17(18):S1565-S1580.
4. Nielsen KJ, Adams DA, Alewood PF, Lewis RJ, Thomas L, Schroeder T, Craik DJ. Effects of chirality at Tyr13 on the structure-activity relationships of omega-conotoxins from Conus magus. *Biochemistry* **1999**;38(21):6741-6751.
5. Adams CM, Kjeldsen F, Zubarev RA, Budnik BA, Haselmann KF. Electron capture dissociation distinguishes a single D-amino acid in a protein and probes the tertiary structure. *Journal of the American Society for Mass Spectrometry* **2004**;15(7):1087-1098.
6. Abo-Riziq AG, Bushnell JE, Crews B, Callahan MP, Grace L, de Vries MS. Discrimination between diastereoisomeric dipeptides by IR-UV double resonance spectroscopy and ab initio calculations. *International Journal of Quantum Chemistry* **2005**;105(4):437-445.
7. Dean JC, Buchanan EG, James WH, Gutberlet A, Biswas B, Ramachandran PV, Zwier TS. Conformation-Specific Spectroscopy and Populations of Diastereomers of a Model Monolignol Derivative: Chiral Effects in a Triol Chain. *Journal of Physical Chemistry A* **2011**;115(30):8464-8478.
8. Gloaguen E, Pagliarulo F, Brenner V, Chin W, Piuzzi F, Tardivel B, Mons M. Intramolecular recognition in a jet-cooled short peptide chain: gamma-turn helicity probed by a neighbouring residue. *Physical Chemistry Chemical Physics* **2007**;9(32):4491-4497.
9. Alauddin M, Gloaguen E, Brenner V, Tardivel B, Mons M, Zehnacker-Rentien A, Declerck V, Aitken DJ. Intrinsic Folding Proclivities in Cyclic b-Peptide Building Blocks:Configuration and Heteroatom Effects Analyzed by Conformer-Selective Spectroscopy and Quantum Chemistry. *Chem. Eur. J.* **2015**;21(on line publication October 5th).
10. Lepere V, Le Barbu-Debus K, Clavaguera C, Scuderi D, Piani G, Simon A-L, Chirot F, MacAleese L, Dugourd P, Zehnacker A. Chirality-dependent structuration of protonated or sodiated polyphenylalanines: IRMPD and ion mobility studies. *Physical chemistry chemical physics : PCCP* **2016**;18(3):1807-17.
11. Sudha R, Jarrold MF. Left-handed and ambidextrous helices in the gas phase. *Journal of Physical Chemistry B* **2005**;109(23):11777-11780.
12. Dunbar RC, Steill JD, Oomens J. Conformations and vibrational spectroscopy of metal-ion/polylalanine complexes. *International Journal of Mass Spectrometry* **2010**;297(1-3):107-115.
13. Dunbar RC, Steill JD, Oomens J. Chirality-Induced Conformational Preferences in Peptide-Metal Ion Binding Revealed by IR Spectroscopy. *Journal of the American Chemical Society* **2011**;133(5):1212-1215.
14. Saavedra CJ, Boto A, Hernandez R, Miranda JI, Aizpurua JM. Conformation and Chiral Effects in alpha,beta,alpha-Tripeptides. *Journal of Organic Chemistry* **2012**;77(14):5907-5913.
15. Vass E, Hollosi M, Besson F, Buchet R. Vibrational spectroscopic detection of beta- and gamma-turns in synthetic and natural peptides and proteins. *Chemical Reviews* **2003**;103(5):1917-1954.
16. Martinek TA, Mandity IM, Fulop L, Toth GK, Vass E, Hollosi M, Forro E, Fulop F. Effects of the alternating backbone configuration on the secondary structure and self-assembly of beta-peptides. *Journal of the American Chemical Society* **2006**;128(41):13539-13544.
17. Kubelka J, Keiderling TA. Differentiation of beta-sheet-forming structures: Ab initio-based simulations of IR absorption and vibrational CD for model peptide and protein beta-sheets. *Journal of the American Chemical Society* **2001**;123(48):12048-12058.
18. Bochicchio B, Tamburro AM. Polyproline II structure in proteins: Identification by chiroptical spectroscopies, stability, and functions. *Chirality* **2002**;14(10):782-792.
19. Eker F, Cao XL, Nafie L, Schweitzer-Stenner R. Tripeptides adopt stable structures in water. A combined polarized visible Raman, FTIR, and VCD spectroscopy study. *Journal of the American Chemical Society* **2002**;124(48):14330-14341.

20. Ducasse L, Castet F, Fritsch A, Huc I, Buffeteau T. Density functional theory calculations and vibrational circular dichroism of aromatic foldamers. *Journal of Physical Chemistry A* **2007**;111(23):5092-5098.
21. Nafie LA, Keiderling TA, Stephens PJ. Vibrational circular-dichroism. *Journal of the American Chemical Society* **1976**;98(10):2715-2723.
22. Stephens PJ. Theory of vibrational circular-dichroism. *Journal of Physical Chemistry* **1985**;89(5):748-752.
23. Freedman TB, Nafie LA, Keiderling TA. VIBRATIONAL OPTICAL-ACTIVITY OF OLIGOPEPTIDES. *Biopolymers* **1995**;37(4):265-279.
24. Blanch EW, Morozova-Roche LA, Cochran DAE, Doig AJ, Hecht L, Barron LD. Is polyproline II helix the killer conformation? A Raman optical activity study of the amyloidogenic prefibrillar intermediate of human lysozyme. *Journal of Molecular Biology* **2000**;301(2):553-563.
25. McColl IH, Blanch EW, Hecht L, Barron LD. A study of alpha-helix hydration in polypeptides, proteins, and viruses using vibrational Raman optical activity. *Journal of the American Chemical Society* **2004**;126(26):8181-8188.
26. Bouchet A, Brotin T, Linares M, Agren H, Cavagnat D, Buffeteau T. Enantioselective Complexation of Chiral Propylene Oxide by an Enantiopure Water-Soluble Cryptophane. *Journal of Organic Chemistry* **2011**;76(10):4178-4181.
27. Heshmat M, Baerends EJ, Polavarapu PL, Nicu VP. The Importance of Large-Amplitude Motions for the Interpretation of Mid-Infrared Vibrational Absorption and Circular Dichroism Spectra: 6,6 '-Dibromo- 1,1 '-binaphthalene -2,2 '-diol in Dimethyl Sulfoxide. *Journal of Physical Chemistry A* **2014**;118(26):4766-4777.
28. Merten C, McDonald R, Xu Y. Strong Solvent-Dependent Preference of Delta and Lambda Stereoisomers of a Tris(diamine)nickel(II) Complex Revealed by Vibrational Circular Dichroism Spectroscopy. *Inorganic Chemistry* **2014**;53(6):3177-3182.
29. Merten C, Li F, Bravo-Rodriguez K, Sanchez-Garcia E, Xu Y, Sander W. Solvent-induced conformational changes in cyclic peptides: a vibrational circular dichroism study. *Physical Chemistry Chemical Physics* **2014**;16(12):5627-5633.
30. Li X, Hopmann KH, Hudecova J, Isaksson J, Novotna J, Stensen W, Andrushchenko V, Urbanova M, Svendsen J-S, Bour P and others. Determination of Absolute Configuration and Conformation of a Cyclic Dipeptide by NMR and Chiral Spectroscopic Methods. *Journal of Physical Chemistry A* **2013**;117(8):1721-1736.
31. Vass E, Strijowski U, Wollschlaeger K, Mandity IM, Szilvagyi G, Jewginski M, Gaus K, Royo S, Majer Z, Sewald N and others. VCD studies on cyclic peptides assembled from L-alpha-amino acids and a trans-2-aminocyclopentane- or trans-2-aminocyclohexane carboxylic acid. *Journal of Peptide Science* **2010**;16(11):613-620.
32. Kim J, Kapitan J, Lakhani A, Bour P, Keiderling TA. Tight beta-turns in peptides. DFT-based study of infrared absorption and vibrational circular dichroism for various conformers including solvent effects. *Theoretical Chemistry Accounts* **2008**;119(1-3):81-97.
33. Moretto A, Crisma M, Formaggio F, Toniolo C, Wu L, Keiderling TA, Kaptein B, Broxterman QB. First homo-peptides undergoing a reversible 3(10)-helix TO alpha-Helix transition. *Biopolymers* **2007**;88(4):556-556.
34. Toniolo C, Formaggio F, Tognon S, Broxterman QB, Kaptein B, Huang R, Setnicka V, Keiderling TA, McColl IH, Hecht L and others. The complete chirospectroscopic signature of the peptide 3(10)-helix in aqueous solution. *Biopolymers* **2004**;75(1):32-45.
35. Silva R, Yasui SC, Kubelka J, Formaggio F, Crisma M, Toniolo C, Keiderling TA. Discriminating 3(10)- from alpha helices: Vibrational and electronic CD and IR absorption study of related Aib-containing oligopeptides. *Biopolymers* **2002**;65(4):229-243.
36. He Y, Bo W, Dukor RK, Nafie LA. Determination of Absolute Configuration of Chiral Molecules Using Vibrational Optical Activity: A Review. *Applied Spectroscopy* **2011**;65(7):699-723.
37. Keiderling TA. Protein and peptide secondary structure and conformational determination with vibrational circular dichroism. *Current Opinion in Chemical Biology* **2002**;6(5):682-688.
38. Kubelka J, Kim J, Bour P, Keiderling TA. Contribution of transition dipole coupling to amide coupling in IR spectra of peptide secondary structures. *Vibrational Spectroscopy* **2006**;42(1):63-73.
39. Berova N, Nakanishi K, Woody RW. Circular Dichroism. Principle and Applications. New York: Wiley; 2000.
40. Baumruck V, Huo DF, Dukor RK, Keiderling TA, Lelièvre D, Brack A. Conformational study of sequential lys-based and leu-based polymers and oligomers using vibrational and electronic CD-spectra *Biopolymers* **1994**;34(8):1115-1121.
41. Buffeteau T, Cavagnat D, Bouchet A, Brotin T. Vibrational absorption and circular dichroism studies of (-)-camphanic acid. *Journal of Physical Chemistry A* **2007**;111(6):1045-1051.
42. Marty R, Frauenrath H, Helbing J. Aggregates from Perylene Bisimide Oligopeptides as a Test Case for Giant Vibrational Circular Dichroism. *Journal of Physical Chemistry B* **2014**;118(38):11152-11160.
43. Moreno JRA, Moreno MMQ, Gonzalez JJL, Claramunt RM, Lopez C, Alkorta I, Elguero J. Self-Assembly Structures of 1H-Indazoles in the Solution and Solid Phases: A Vibrational (IR, FIR, Raman, and VCD) Spectroscopy and Computational Study. *Chemphyschem* **2013**;14(14):3355-3360.
44. Sinha S, Srivastava R, De Clereq E, Singh RK. Synthesis and antiviral properties of arabino and ribonucleosides of 1,3-dideazaadenine, 4-nitro-1,3-dideazapurine and diketopiperazine. *Nucleosides Nucleotides & Nucleic Acids* **2004**;23(12):1815-1824.
45. Grande F, Garofalo A, Neamati N. Small molecules anti-HIV therapeutics targeting CXCR4. *Current Pharmaceutical Design* **2008**;14(4):385-404.
46. Martins MB, Carvalho I. Diketopiperazines: biological activity and synthesis. *Tetrahedron* **2007**;63(40):9923-9932.
47. Nicholson B, Lloyd GK, Miller BR, Palladino MA, Kiso Y, Hayashi Y, Neuteboom STC. NPI-2358 is a tubulin-depolymerizing agent: in-vitro evidence for activity as a tumor vascular-disrupting agent. *Anti-Cancer Drugs* **2006**;17(1):25-31.
48. Berset J-D, Ochsenbein N. Stability considerations of aspartame in the direct analysis of artificial sweeteners in water samples using high-performance liquid chromatography-tandem mass spectrometry (HPLC-MS/MS). *Chemosphere* **2012**;88(5):563-569.
49. Lin SY, Cheng YD. Simultaneous formation and detection of the reaction product of solid-state aspartame sweetener by FT-IR/DSC microscopic system. *Food Additives and Contaminants Part a-Chemistry Analysis Control Exposure & Risk Assessment* **2000**;17(10):821-827.
50. Lin SY, Wang SL. Advances in simultaneous DSC-FTIR microspectroscopy for rapid solid-state chemical stability studies: Some dipeptide drugs as examples. *Advanced Drug Delivery Reviews* **2012**;64(5):461-478.
51. Borthwick AD. 2,5-Diketopiperazines: Synthesis, Reactions, Medicinal Chemistry, and Bioactive Natural Products. *Chemical Reviews* **2012**;112(7):3641-3716.

52. Capasso S, Vergara A, Mazzarella L. Mechanism of 2,5-dioxopiperazine formation. *Journal of the American Chemical Society* **1998**;120(9):1990-1995.
53. Basiuk VA, Gromovoy TY. THE GAS SOLID-PHASE 2,5-DIOXOPIPERAZINE SYNTHESIS - CYCLIZATION OF VAPOROUS DIPEPTIDES ON SILICA SURFACE. *Collection of Czechoslovak Chemical Communications* **1994**;59(2):461-466.
54. Corey RB. The Crystal Structure of Diketopiperazine. *Journal of the American Chemical Society* **1938**;60:1598−1604.
55. Karle IL. X-Ray Analysis: Conformation of Peptides in the Crystalline State. In: Gross E, editor. The Peptides Analysis, Synthesis, Biology

Modern Techniques of Conformational Structural, and Configurational Analysis. Volume 4: Elsevier; 1981. p 1-54.

56. Kopple KD, Marr DH. Conformation of cyclic peptides. The folding of cyclic dipeptides containing an aromatic side chain. *Journal of the American Chemical Society* **1967**;89(24):6193-200.
57. Lin C-F, Webb LE. Crystal structures and conformations of the cyclic dipeptides cyclo-(Glycyl-L-tyrosyl) and cyclo-(L-seryl-L-tyrosyl) Monohydrate. *Journal of the American Chemical Society* **1973**;95(20):6803-11.
58. Benedetti E, Marsh RE, Goodman M. Conformational studies on peptides. X-ray structure determinations of six N-methylated cyclic dipeptides derived from alanine, valine, and phenylalanine. *Journal of the American Chemical Society* **1976**;98(21):6676-84.
59. Hooker TM, Jr., Bayley PM, Radding W, Schellman JA. The optical properties of alanine and proline diketopiperazines. *Biopolymers* **1974**;13(3):549-66.
60. Matile S, Berova N, Nakanishi K, Novkova S, Philipova I, Blagoev B. PORPHYRINS - POWERFUL CHROMOPHORES FOR STRUCTURAL STUDIES BY EXCITON-COUPLED CIRCULAR-DICHROISM. *Journal of the American Chemical Society* **1995**;117(26):7021-7022.
61. Berova N, Di Bari L, Pescitelli G. Application of electronic circular dichroism in configurational and conformational analysis of organic compounds. *Chemical Society Reviews* **2007**;36(6):914-931.
62. Taniguchi T, Monde K. Exciton Chirality Method in Vibrational Circular Dichroism. *Journal of the American Chemical Society* **2012**;134(8):3695-3698.
63. Abbate S, Mazzeo G, Meneghini S, Longhi G, Boiadjiev SE, Lightner DA. Bicamphor: A Prototypic Molecular System to Investigate Vibrational Excitons. *Journal of Physical Chemistry A* **2015**;119(18):4261-4267.
64. Covington CL, Nicu VP, Polayarapu PL. Determination of the Absolute Configurations Using Exciton Chirality Method for Vibrational Circular Dichroism: Right Answers for the Wrong Reasons? *Journal of Physical Chemistry A* **2015**;119(42):10589-10601.
65. Nicu VP, Domingos SR, Strudwick BH, Brouwer AM, Buma WJ. Interplay of Exciton Coupling and Large-Amplitude Motions in the Vibrational Circular Dichroism Spectrum of Dehydroquinidine. *Chemistry-a European Journal* **2016**;22(2):704-715.
66. Nicu VP. Revisiting an old concept: the coupled oscillator model for VCD. Part 1: the generalised coupled oscillator mechanism and its intrinsic connection to the strength of VCD signals. *Physical Chemistry Chemical Physics* **2016**;18(31):21202-21212.
67. Perez-Mellor AF, Alata I, Lepère V, Zehnacker A. **Manuscript in preparation**.
68. Nitecki DE, Halpern B, Westley JW. Simple route to sterically pure diketopiperazines. *The Journal of organic chemistry* **1968**;33(2):864-6.
69. Jeziorna A, Stopczyk K, Skorupska E, Luberda-Durnas K, Oszajca M, Lasocha W, Gorecki M, Frelek J, Potrzebowski MJ. Cyclic Dipeptides as Building Units of Nano- and Microdevices: Synthesis, Properties, and Structural Studies. *Crystal Growth & Design* **2015**;15(10):5138-5148.
70. Le Barbu-Debus K, Broquier M, Mahjoub A, Zehnacker-Rentien A. Chiral recognition in jet-cooled complexes of (1R,2S)-(+)-cis-1-amino-2-indanol and methyl lactate: on the importance of the CH center dot center dot center dot pi interaction. *Physical Chemistry Chemical Physics* **2009**;11(35):7589-7598.
71. Scuderi D, Le Barbu-Debus K, Zehnacker A. The role of weak hydrogen bonds in chiral recognition. *Physical Chemistry Chemical Physics* **2011**;13(40):17916-17929.
72. Merten C, Kowalik T, Hartwig A. Vibrational circular dichroism spectroscopy of solid polymer films: Effects of sample orientation. *Applied Spectroscopy* **2008**;62(8):901-905.
73. Buffeteau T, Lagugne-Labarthet FS, Sourisseau C. Vibrational circular dichroism in general anisotropic thin solid films: Measurement and theoretical approach. *Applied Spectroscopy* **2005**;59(6):732-745.
74. MacroModel version 9.8; ed. Schrödinger, LLC: New York, NY, 2010. *MacroModel version 9.8; ed. Schrödinger, LLC: New York, NY, 2010* **2010**.
75. Grimme S, Antony J, Ehrlich S, Krieg H. A consistent and accurate ab initio parametrization of density functional dispersion correction (DFT-D) for the 94 elements H-Pu. *Journal of Chemical Physics* **2010**;132(15).
76. Frisch MJ, Trucks GW, Schlegel HB, Scuseria GE, Robb MA, Cheeseman JR, Scalmani G, Barone V, Mennucci B, Petersson GA and others. Gaussian 09, Revision D.01. Wallingford CT: Gaussian Inc.; 2009.
77. Gdaniec M, Liberek B. STRUCTURE OF CYCLO(-L-PHENYLALANYL-L-PHENYLALANYL-). *Acta Crystallographica Section C-Crystal Structure Communications* **1986**;42:1343-1345.
78. Li XJ, Hopmann KH, Hudecova J, Stensen W, Novotna J, Urbanova M, Svendsen JS, Bour P, Ruud K. Absolute Configuration of a Cyclic Dipeptide Reflected in Vibrational Optical Activity: Ab Initio and Experimental Investigation. *Journal of Physical Chemistry A* **2012**;116(10):2554-2563.
79. Anet FAL, Miura SS, Siegel J, Mislow K. La Coupe du Roi and Its Relevance to Stereochemistry. Combination of Two Homochiral Molecules To Give an Achiral Product. *Journal of the American Chemical Society* **1983**;105(6):1419-1426.
80. Altnoeder J, Bouchet A, Lee JJ, Otto KE, Suhm MA, Zehnacker-Rentien A. Chirality-dependent balance between hydrogen bonding and London dispersion in isolated (+-)-1-indanol clusters. *Physical Chemistry Chemical Physics* **2013**;15:10167-10180.
81. Urbanova M, Setnicka V, Devlin FJ, Stephens PJ. Determination of molecular structure in solution using vibrational circular dichroism spectroscopy: the supramolecular tetramer of S-2,2 '-dimethyl-biphenyl-6,6 '-dicarboxylic acid. *Journal of the American Chemical Society* **2005**;127(18):6700-6711.

Tables

Experimental frequency (cm^{-1})	Calculated frequency (cm^{-1})*	Dipole strengths $\times10^{-40}$ / Rotational strengths $\times10^{-44}$ ($esu^2 \cdot cm^2$)	Angle between electric and magnetic dipole transition moments (degree)	Assignment
1092	1123	93 / 2	89	Aromatic β(CH) bends
	1129	87 / 0	90	
1326	1295	101/ -36	98	Aliphatic (DKP ring) β(CH)
1340	1347	248 / 40	86	
1350	1350	136 / -3	91	
	1366	71 / 21	83	
1452	1464	689 / 59	88	Free β(NH) bends mixed with DKP ring β(CH) bend carbon in α
1462	1482	378 / -150	99	
	1569	98 / 8	86	Symmetric bound β(NH) bend
	1580	15 / -17	94	Antisymmetric bound β(NH) bend
1650	1733	17 / 39	79	Symmetric bound ν(CO) stretch (coupled to symmetric β (NH) bend)
1663	1762	1930 / 296	86	Antisymmetric bound ν(CO) stretch (coupled to antisymmetric β (NH) bend)
1677	1787.7	606 / -104	93	Free ν(CO) stretches coupled to adjacent free β (NH) bend
	1788.3	592 / -171	97	
3152	3227	284 / -35	91	Symmetric bound ν(NH) stretch
3205	3291	1724 / 427	87	Antisymmetric bound ν(NH) stretch
3314	3586	39 / 14	86	Free ν(NH) stretches
	3597	27 / -23	104	

Table I: Frequencies assignment for cyclo LPhe-LPhe. (*) The theoretical frequencies are not scaled. The position of experimental frequencies were calculated using second derivative criterion.

Graphical Abstract